Thermal Properties and Fire Resistance of Cement Base Material for Road Pavement Based on Finite Element Analysis

Chenglong Ma

Zhejiang Tongji Vocational College of Science and Technology, Hangzhou 311231, China

Corresponding Author Email: mcL1971@126.com

ABSTRACT

The physical and chemical properties of cement base material for road pavement will undergo changes in high temperature environment, so improving the high temperature resistance and fire resistance of cement base material is very important for reducing the loss of road projects caused by high temperature. In actual engineering projects, maintenance measures are often adopted to repair the damaged components so that the roads could be used continuously, however, research on the thermal properties and fire resistance of cement base components of road pavement is insufficient, therefore, in view of this blank, this paper aims to study the thermal properties and fire resistance of road cement base material based on finite element analysis. At first, this paper measured the temperature inside the road cement base during the process of environmental thermal fatigue, analyzed the law of the response of cement base to the temperature changes under the action of relative humidity in the micro environment, and figured out the delay time of such response and the changes of internal temperature gradient. Then, this paper selected proper thermal parameters of road cement material and the stress-strain relationship under compression or tension in high temperature environment, and used the software Python to perform finite element analysis on the fire resistance of road cement base specimens. At last, the corresponding experimental results were given and the validity of the constructed model was verified.

1. INTRODUCTION

Good resistance to wear, frost, fire, and explosion is necessary for cement base material used for the pavement of roads, highways, airport runways and other projects [1-6], however, under high temperature, road cement base material is prone to temperature stress [7-11], for mortar, concrete, grout, and other building materials that take cement as the cementing material, their thermal expansion coefficients are different, as the temperature changes, the different deformations would result in temperature stress inside the structure of road cement base, and when the stress concentration reaches a certain value, the structure of road cement base will crack, which is detrimental to the construction quality of road structure [12-19]. Moreover, under high temperature, the physical and chemical properties of road cement base will undergo changes, such as mass reduction, formation of holes and cracks, and the decline of stress and durability performance [20-23]. Therefore, improving the high temperature resistance and fire resistance of road cement base material is very important for reducing the economic loss of road projects caused by high temperature.

Under high temperature, the sealing integrity of cement sheath in offshore oil wells will be seriously threatened, which can lead to problems such as gas channeling, to provide more experimental results, Zou et al. [24] prepared and analyzed samples of a cement slurry sealing section of a typical offshore high-temperature well, and evaluated the mechanical

properties with a triaxial pressure servo instrument and a high-temperature curing kettle; the researchers also tested the density and the Poisson's ratio of the samples and plotted the stress-strain curve to attain the elastic modulus and the compressive strength. Gunjal and Kondraivendhan [25] used calcined clay-limestone cement to prepare concrete, compared it with concrete using ordinary portland cement of grade 53, and tested its physical and chemical properties, the attained results showed that, the compressive strength decreased after the temperature rose to 200°C and significant losses occurred after 400°C, then noticeable minute cracks started to appear on the surface of the cube specimens. Duarte et al. [26] experimented on the fire behaviour of GFRP-reinforced concrete slab strips and performed numerical investigations. The researchers tested the fire resistance of four concrete slab strips reinforced with sand-coated GFRP bars in a four-point bending configuration, the specimens were subjected to a sustained service load and their bottom surface was exposed to the ISO 834 fire curve. The tests were then complemented with the development of 3D thermo-mechanical finite element models of the slab strips to simulate the fire resistance tests. The test results showed that specimens manufactured with a higher concrete strength presented less extensive cracking, reducing the localized heating of the reinforcement and leading to a higher fire resistance. Ye et al. [27] built a robust finite element model in ABAQUS to study the performance of steel-concrete composite joints in post-earthquake fire scenarios and verified the model using the results of previous

experiments, then they carried out comprehensive numerical analysis and identified the parameters affecting the post-earthquake fire behavior of the steel-concrete composite joints.

According to the existing research findings, world field scholars have made some comparisons of the cement base material for road pavement at room temperature and high temperature, however, due to the high cost and difficult operation of open fire test of road cement base components and the fact that the actual project usually takes repair measures to repair the damaged components, and this can also realize uninterrupted use of roads, so the analysis of the thermal properties and fire resistance of road cement base components is insufficient. Therefore, in view of this blank, this paper studied the thermal properties and fire resistance of cement base material for road pavement based on finite element analysis. In the second chapter, the internal temperature of road cement base during the process of environmental thermal fatigue was measured, the law of the response of cement base material to temperature changes under the action of relative humidity in the micro environment was analyzed, and the delay time of such response and the changes of internal temperature gradient were figured out. In the third chapter, this paper selected proper thermal parameters of road cement material and the stress-strain relationship under compression or tension in high temperature environment, and used Python to perform finite element analysis on the fire resistance of road cement base specimens. At last, the corresponding experimental results were given and the validity of the constructed model was verified.

2. RESPONSE OF THE INTERNAL TEMPERATURE OF ROAD CEMENT BASE TO AMBIENT TEMPERATURE

To reveal the evolution mechanism of the performance of road cement base under high ambient temperature, in this paper, the difference between the ambient temperature and the internal temperature of road cement base, as well as the relative humidity of the micro environment were changed to explore the law of changes of the internal temperature response of road cement base. At first, the temperature inside the road cement base during the process of environmental thermal fatigue was measure; then, the law of such response under the action of relative humidity in the micro environment was analyzed to attain the delay time of the response and the changes of internal temperature gradient.

To study the internal temperature response of road cement base, this paper adopted the one-dimensional heat conduction temperature solution to analyze the changes of the internal temperature gradient of road cement base material. Assuming: $\omega(a, \varphi)$ represents the excess temperature of a certain position of the road cement base at a certain time moment; ω_0 represents the excess temperature of the initial time moment; o_0 represents the initial internal temperature of the road cement base; o_p represents the ambient temperature, there is $\omega_0 = o_0 - o_p$; γ_m represents the root of the transcendental equation $tan(\gamma_m\xi) = Y_i/\gamma_m\xi$, $\gamma_m\xi$ represents the function of a dimensionless number Y_i, Y_i represents the Biot number and it satisfies $Y_i = f\xi/\mu$; $x\varphi/\xi^2$ is also a dimensionless number, a/ξ represents the dimensionless coordinates; let Fourier number G_0 be equal to $x\varphi/\xi^2$, then the following formula gives the temperature solution of the one-dimensional transient heat conduction problem:

$$\frac{\omega(a, \phi)}{\omega_o} = 2p^{-(\gamma_1\xi)^2\left(\frac{x\phi}{\xi^2}\right)}$$
$$\cdot \frac{\sin(\gamma_m\xi) \cdot \cos\left[(\gamma_m\xi) \cdot \left(\frac{a}{\xi}\right)\right]}{\gamma_m\xi + \sin(\gamma_m\xi)\cos(\gamma_m\xi)} \quad (1)$$

When the Fourier number G_0 is greater than 0.2, the above formula converges faster. By comparing the results calculated based the first term of the series and the complete series, it's found that the difference between the two calculation results was very small, so the above formula can be simplified as follows:

$$\frac{\omega(a, \phi)}{\omega_0} = 2p^{-(\gamma_1\xi)^2\left(\frac{x\phi}{\xi^2}\right)}$$
$$\cdot \frac{\sin(\gamma_1\xi) \cdot \cos\left[(\gamma_1\xi) \cdot \left(\frac{a}{\xi}\right)\right]}{\gamma_1\xi + \sin(\gamma_1\xi)\cos(\gamma_1\xi)} \quad (2)$$

By substituting $\omega(a,\varphi) = o(a,\varphi) - o_p$ and $\omega_0 = o_0 - o_p$ into the above formula, the temperature at any position of the road cement base at any time moment could be calculated based on the following formula:

$$o(a, \phi) = o_p + 2(o_0 - o_p)p^{-(\gamma_1\xi)^2\left(\frac{x\phi}{\xi^2}\right)}$$
$$\cdot \frac{\sin(\gamma_1\xi) \cdot \cos\left[(\gamma_1\xi) \cdot \left(\frac{a}{\xi}\right)\right]}{\gamma_1\xi + \sin(\gamma_1\xi)\cos(\gamma_1\xi)} \quad (3)$$

By taking the derivative of a in the above formula, the temperature gradient inside the road cement base could be attained:

$$\frac{\partial o(a, \phi)}{\partial a} = -2\gamma_1(o_0 - o_p)p^{-(\gamma_1\xi)^2\left(\frac{x\phi}{\xi^2}\right)}$$
$$\cdot \frac{\sin(\gamma_1\xi) \cdot \cos\left[(\gamma_1\xi) \cdot \left(\frac{a}{\xi}\right)\right]}{\gamma_1\xi + \sin(\gamma_1\xi)\cos(\gamma_1\xi)} \quad (4)$$

By taking the second derivative of a in the above formula, we have:

$$\frac{\partial^2 o(a, \phi)}{\partial a^2} = -2\gamma_1^2(o_0 - o_p)p^{-(\gamma_1\xi)^2\left(\frac{x\phi}{\xi^2}\right)}$$
$$\cdot \frac{\sin(\gamma_1\xi) \cdot \cos\left[(\gamma_1\xi) \cdot \left(\frac{a}{\xi}\right)\right]}{\gamma_1\xi + \sin(\gamma_1\xi)\cos(\gamma_1\xi)} \quad (5)$$

The development law of the internal temperature rise rate of road cement base can be explained by the position at which the maximum value of $\partial^2 o^2/\partial a^2$ appears, according to above formula, at the initial moment, the value of $\partial^2 o^2/\partial a^2$ was the largest, then, with the increase of the duration of high ambient temperature, this value decreased, so it can be inferred that the main cause of the changes in the internal temperature rise of the road cement base is the changes of the temperature gradient. At the same time, the greater the value of $o_0 - o_p$, the faster the internal temperature rise of the road cement base.

3. FINITE ELEMENT ANALYSIS OF THE FIRE RESISTANCE OF ROAD CEMENT BASE

The heat transfer caused by high ambient temperature will

lead to an uneven temperature field in the section of road cement base components, resulting in changes in the strength and deformation of the road cement base material. In order to get the distribution law of temperature field on the section of road cement base material and the changes of the deformation of the road cement base, it's a necessary work to sort out and analyze the test results of road cement base components obtained by previous researchers, and figure out the thermal parameters of the road cement base material and the mechanical parameters of the ambient temperature, so as to lay a good foundation for the construction of the finite element model of the road cement base components. Besides, another more important thing is to figure out the stress-strain relationship of the road cement base under tension in high temperature environment. Figure 1 gives the flow of the finite element model.
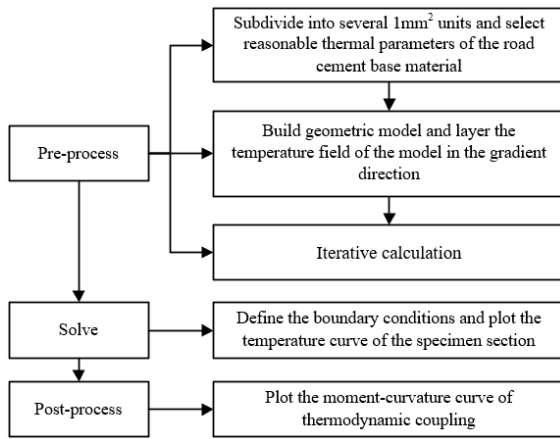

Figure 1. Flow of the finite element model

To select proper thermal parameters of road cement base material and stress-strain relationship under compression or tension in high temperature environment, the software *Python* was adopted to perform finite element analysis on the fire resistance of specimens of road cement base. In this paper, $0.1s$ was defined as the time step, within each time step, the created scenario of high temperature environment, the heat transfer and stress on the section of the road cement base specimens under fire were analyzed.

At first, the created high temperature environment scenario was analyzed. Key step of the research on the fire resistance of road cement base specimens was the selection of the temperature-time curve of road cement base material. The commonly-used *ISO* 834 temperature rise curve is given by the following formula:

$$O = O_0 + 345 \lg(8o + 1) \qquad (6)$$

Assuming: O_0 represents the initial ambient temperature, O represents the ambient temperature after time duration o, o represents the duration of fire, then the commonly-used *ASTM E*119 temperature rise curve is given by the following formula:

$$O = O_0 + 750\left[1 - \exp\left(-3.79553\sqrt{o/60}\right)\right] + 180.41\sqrt{o/60} \qquad (7)$$

Under current standards, although the above two temperature rise curves have been widely used in studies on the fire resistance performance of road cement base specimens,

however, they cannot accurately reflect the actual conditions of flame combustion in high temperature environment, this is because in an actual high temperature environment, the flame will tend to extinguish in the later stage of combustion, and in the stage of combustion intensity weakening, part of the strength and rigidity inside the road cement base material will restore, and the above two temperature rise curves cannot describe the fire resistance of the specimens at this time. Therefore, for this stage, the *ISO* 834 temperature rise curve shown in the following formula was considered, assuming: O_f and o_f represent the temperature and time at which the ambient temperature begins to fall, then there are:

$$O = \begin{cases} O_f - 10.417(o - o_f), o_f \leq 30\,\mathrm{min} \\ O_f - 4.167\left(3 - \dfrac{o_f}{60}\right)(o - o_f), 30\,\mathrm{min} < o_f \leq 120\,\mathrm{min} \\ O_f - 4.167(o - o_f), o_f > 120\,\mathrm{min} \end{cases} \qquad (8)$$
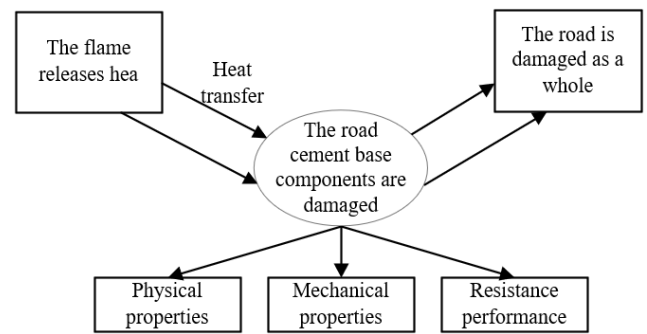

Figure 2. The heat transfer process of road cement base specimens in high temperature environment

Then, the heat transfer on the specimen section was analyzed, that is, the temperature distribution on the specimen section was calculated. The transfer of heat has three forms: heat conduction, heat convection, and heat radiation. During the fire resistance test, in the high temperature furnace, the heat flux first reaches the outermost surface of the specimen, and then exchanges heat with the specimen surface through heat convection and heat radiation. Then, when the heat flux reaches the inside of the specimen, it exchanges heat with the inside of the specimen through heat conduction. Figure 2 shows the heat transfer process of road cement base specimens in high temperature environment. Assuming: l represents the coefficient of heat conduction, W represents the amount of heat produced by per unit volume of the road cement base specimen within per unit time, this paper constructed a Fourier differential equation to describe the temperature gradient distribution on the section of road cement base specimens under the form of heat conduction:

$$l\nabla^2 O + W = \sigma d \frac{\partial O}{\partial o} \qquad (9)$$

For the convenience of calculation, it's assumed that the road cement base specimen itself does not produce inherent heat, that is, W is equal to 0. The heat convection and heat radiation processes of the heat exchange between heat flux and the outermost surface of road cement base specimens can be described by the following formula, assuming: m represents the outer normal direction of the surface of the road cement base specimen, f_d represents the coefficient of heat convection,

O_g represents the calculated flame temperature of the fire, O_n represents the surface temperature of the road cement base specimen, ρ_n represents the radiation coefficient of the surface of the road cement base specimen, ρ_g represents the radiation coefficient of the flame, ε represents the Boltzmann constant, then there is:

$$l\frac{\partial O}{\partial m} = f_d(O_g - O_n) \\ + \varepsilon\rho_n\rho_g\left[(O_g + 273.14)^4 \right. \quad (10) \\ \left. - (O_n + 273.15)^4\right]$$

The road cement base specimens were subject to heat transfer analysis based on the temperature calculated from the temperature rise curves. At first, the section of specimens was sub-divided into several $1mm^2$ units, proper thermal parameters of the road cement base material were selected, and the constructed differential equation of heat transfer was solved. Then, based on the solution of the equation, the temperature curve of each section of the specimens could be plotted.

At last, the mechanical performance of specimen section under fire was analyzed to figure out the moment-curvature relationship of the specimen section. By combining the section temperature attained from the heat transfer analysis with the stress-strain relationship of the road cement base material in high temperature environment under compression and tension, the said mechanical performance of specimen section could be analyzed. High temperature environment can seriously affect the mechanical properties of road cement base material. Assuming: ρ_{tot} represents the total strain, ρ_F represents the mechanical strain, ρ_T represents the temperature strain, the following formula gives the strain relationship of the road cement base material:

$$\rho_{Total} = \rho_F + \rho_T \quad (11)$$

This paper adopted the plane section assumption for the calculation of the mechanical performance of specimen section under fire, the total strain of the specimen section was determined by the area of the section of the specimen, and it's not affected by the temperature of the section. The temperature strain affected by the temperature of specimen can be attained by integrating the thermal expansion coefficient of the road cement base material.

The shear force was ignored during the analysis, so when the specimen was subject to stress and bent, the specimen section still met the plane section assumption. Besides, the analysis process also ignored the peeling of the road cement base in high temperature environment. Assuming: ε_d represents the stress of the road cement base, X represents the area of the section, c_{ri} represents the distance from the center of the i-th unit to the neutral axis of the specimen section, the following formula gives the expression of the axial force and moment balance conditions satisfied by the finite element analysis of the road cement base specimen section:

$$M = \iint_X \varepsilon dX \cong \sum_X \varepsilon_d X_{ij} \quad (12)$$

$$N = \iint_X \varepsilon c dX \cong \sum_X \varepsilon_d c_i X_{ij} \quad (13)$$

The above equation needs to be solved based on iterative program. That is, to determine a strain value and a curvature at the center of specimen section, and then calculate its stress value based on the stress-strain relationship of the road cement base material in high temperature environment under compression and tension. After that, using the iterative program, the stress under different strain values was iteratively calculated to attain the strain that meets the force balance condition and the stress corresponding to this strain, based on this attained strain and the above formula, we can easily calculate the bending moment of the road cement base specimen corresponding to the selected curvature.

After above steps were completed, the deflection of the specimen was further calculated based on the plotted thermo-mechanical coupling moment-curvature curve according to the principle of virtual work. Assuming: o_H represents the duration of the fire, ρ_ε represents the strain caused by the real load, and they satisfy $\varepsilon_\varepsilon = g(N, M, o_H...)$; Ψ represents the curvature caused by the real load and there is $\Psi = g(M, N, o_H...)$; g represents the virtual force, Ψ is the bending moment of the specimen under fire duration o_H, $\Psi = g(N)$ represents the curvature curve, the following formula gives the expression of the virtual work principle of specimens considering normal force and bending moment:

$$g \cdot u = \int_K (M \cdot \rho_\varepsilon + N \cdot \Psi) da \quad (14)$$

If the specimen $M=0$, then the above formula can be simplified as:

$$g \cdot u = \int_K N \cdot \Psi da \quad (15)$$

To solve the equation, the above formula needs to be discretized, then there is:

$$g \cdot u = \sum_i N_i \cdot \Psi_i(N_i) \cdot \Delta a_i \quad (16)$$

Based on above formula, the deflection at any position of the specimen at any time step can be calculated.

4. EXPERIMENTAL RESULTS AND ANALYSIS

Table 1 shows the experimental results of the internal temperature rise rate of road cement base specimens. According to the data in the table, the evolution laws of the three specimens are basically consistent. Under the condition of a same temperature difference, the internal temperature of the specimens exhibited the largest rise rate during the early stage; then it decreased gradually during the transition stage and reached the smallest in the later stage. After that, this paper compared the solutions of the temperature field of 9 measuring points attained in this paper with their analytical solutions, and the comparison results are given in Table 2, as can be seen in the table, the differences between the attained solutions and the analytical solutions are small, and the maximum error is 0.152, which has verified the validity and calculation accuracy of the finite element analysis method proposed in this paper.

Based on the selection of different measuring points of different specimens, the temperature-time curves of the surface and inside of the specimens could be plotted to further analyze the temperature evolution laws of different positions

on the section of the specimens. Figure 3 and Figure 4 show the temperature-time curves of different specimens and the temperature-time curves of different measuring points on a same specimen.

Table 1. Experimental results of the internal temperature rise rate of road cement base specimens

Specimen No.	Depth	Rise rate in early stage	Rise rate in transition stage	Rise rate in later stage
	30	1.43	0.416	0.025
1	60	1.25	0.037	0.037
	90	0.96	0.283	0.060
	30	2.41	0.192	0.025
2	60	1.74	0.286	0.026
	90	1.33	0.235	0.045
	30	1.82	0.140	0.018
3	60	1.51	0.195	0.032
	90	1.16	0.243	0.053

Table 2. Comparison results of the attained solutions and analytical solutions of different measuring points

Coordinates	Attained solution	Analytical solution	Relative error
(10, 10)	219.2732	219.2883	0.0069
(20, 20)	228.2126	228.2375	0.0109
(30, 30)	227.0881	227.1186	0.0134
(40, 40)	217.7284	217.7593	0.0141
(50, 50)	202.3442	202.3751	0.0152
(60, 60)	183.0671	183.0936	0.0144
(70, 70)	161.7645	161.7858	0.0131
(80, 80)	140.0083	140.0221	0.0099
(90, 90)	119.0771	119.0853	0.0069

As can be seen from the figure, the simulated curves shown in Figures 3 and 4 are smooth because situations such as cracking of the road cement base material had been ignored. Due to the existence of a hot air transition layer, the ambient temperature was always higher than the surface temperature of the specimens, and the temperature difference between the two gradually decreased as the high temperature continued. After 100min, the temperature curve of the measuring points on the direct fire surface peaked, which was consistent with the reference curve of criterion. The temperature curves of the measuring points on the surface not facing the fire exhibited as straight lines, and the slope of the straight line was the ratio of the final temperature of the measuring point to the distance

from its position to the flame. Thus, the conclusion can be drawn as that: the closer the measuring point to the flame, the greater the temperature rise rate during the fire resistance experiment of the specimens.
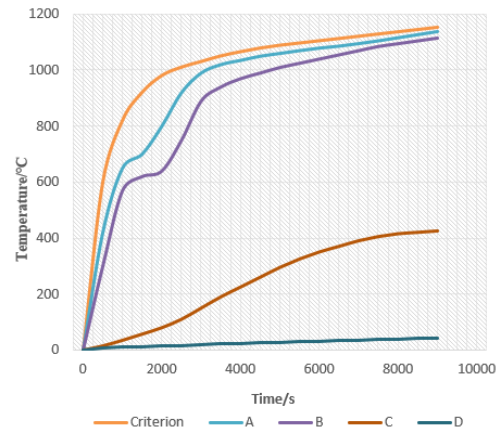

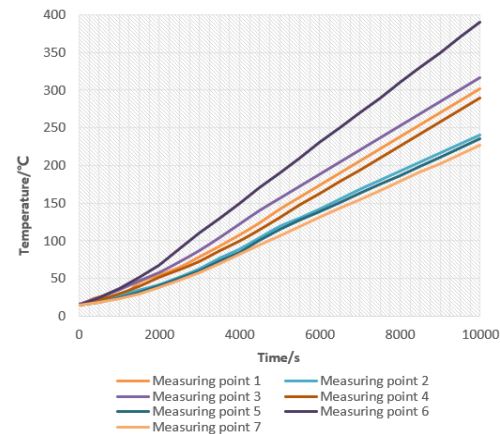**Figure 3.** Temperature-time curves of different specimens

Figure 4. Temperature-time curves of different measuring points on a same specimen

Then, this paper discussed the convergence problem of finite element analysis. The discretization of specimens was realized based on 4-node PLANE13 plane thermal coupling units. The standardized stress of different measuring points under different grid sizes and different layer numbers was calculated, and the experimental results are shown in Table 3 and Table 4.

Table 3. Results of standard thermal stress finite element analysis at point C

Size	Layer number 5	15	25	35	45	Reference solution
1	-0.02227	-0.22853	-	-	-	
0.6	-0.03023	-0.23681	-0.24625	-	-	-0.25153
0.3	-0.03212	-0.23882	-0.24816	-0.25253	-	
0.1	-0.03264	-0.23936	-0.24875	-0.25212	-0.25134	

Table 4. Results of standard thermal stress finite element analysis at point D

Size	Layer number 5	15	25	35	45	Reference solution
1	2.74365	2.09633	-	-	-	
0.6	2.68532	2.05426	2.04852	-	-	2.01937
0.3	2.67081	2.04371	2.03804	2.03654	-	
0.1	2.66673	2.04082	2.03509	2.03351	2.01642	

According to the table, with the decrease of grid size and the increase of layer number, the thermal stress of measuring points of the road cement base material gradually converged to the reference solution of finite element analysis. The increase of layer number can significantly improve the convergence rate of the analytical model, so when building the finite element analysis model, a reasonable number of layers should be set.

Figure 5 and Figure 6 show the vertical displacement-time curves of measuring points that are far from the flame. As can be seen from the figures, for measuring points on different positions of the specimen, during the temperature rise process, the vertical displacement of measuring points far from the flame changed in the same pace, the change rate was slow, and the maximum displacement during the later stage of temperature rise was still less than 50cm. For measuring points that were closer to the flame, there were great differences in their vertical displacement, the changes of some measuring points were large and the change rate was fast, the shorter distance decreased the area of the compression zone of the road cement base material, and greatly increased the vertical displacement.
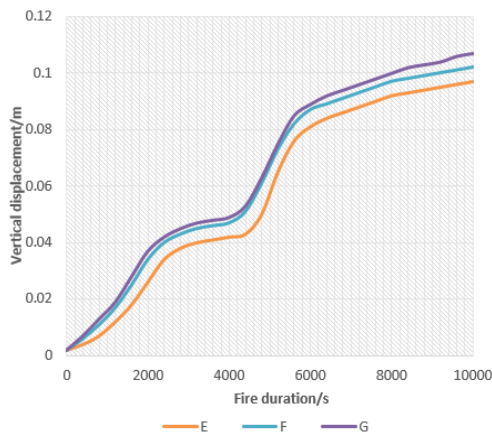

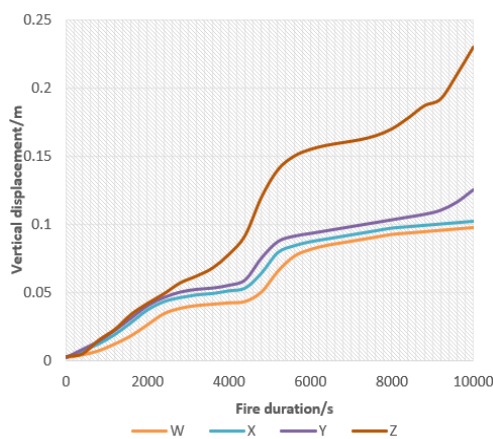**Figure 5.** Vertical displacement - fire duration curves of measuring points far away from the flame

Figure 6. Vertical displacement - fire duration curves of measuring points close to the flame

5. CONCLUSION

This paper analyzed the thermal performance of road cement base material based on finite element analysis and verified its fire resistance. At first, the internal temperature of the road cement base material during fatigue process in the high temperature environment was measured, the law of the response of cement base to temperature changes under the action of relative humidity in the micro environment was analyzed, the delay time of such response and the changes of internal temperature gradient were studied. Then, the paper selected proper thermal parameters of road cement base material and stress-strain relationship under compression or tension in high temperature environment, and performed finite element analysis on the fire resistance of specimens of road cement base in *Python*.

After that, experiments were performed to measure the internal temperature rise rate of road cement base specimens, the attained solutions and analytical solutions of the temperature field at 9 measuring points were compared, the validity and calculation accuracy of the finite element analysis method proposed in this paper were verified. Moreover, this paper gave the temperature-time curves of different specimens and the temperature-time curves of different measuring points on a same specimen, and drew the conclusion that the closer the measuring point to the flame, the greater the temperature rise rate during the fire resistance experiment. At last, the standard stress of different measuring points under different grid sizes and layer numbers was calculated, the vertical displacement-fire duration curves of measuring points far from the flame were plotted, and the corresponding analysis results were given.

REFERENCES

[1] He, B., Xu, J. (2021). The application of simultaneous paver liquid cement sprinkling system in the road construction of Yun-Mao Highway. In E3S Web of Conferences, 233: 01135. https://doi.org/10.1051/e3sconf/202123301135

[2] Dave, N., Sahu, V., Misra, A.K. (2020). Development of geopolymer cement concrete for highway infrastructure applications. Journal of Engineering, Design and Technology, 18(5): 1321-1333. https://doi.org/10.1108/JEDT-10-2019-0263

[3] Teijón-López-Zuazo, E., Vega-Zamanillo, Á., Calzada-Pérez, M.Á., Juli-Gándara, L. (2020). Estimation of unconfined compressive strength of cement-stabilized jabre as material upgrade on highway construction. Materiales de Construcción, 70(338): e218-e218.

[4] Feng, R., Wu, L., Liu, D., Wang, Y., Peng, B. (2020). Lime-and cement-treated sandy lean clay for highway subgrade in China. Journal of materials in civil engineering, 32(1): 04019335. https://doi.org/10.1061/(ASCE)MT.1943-5533.0002984

[5] Zhu, J.P., Zhang, J.H., Wang, P., Cheng, Y.W., Lou, P. (2020). Numerical simulation of settlement of cement-soil mixing pile subgrade of large-scale soft soil first-class highway. Journal of Railway Science and Engineering, 17(6): 1390-1395.

[6] Edeh, J.E., Ugama, T., Okpe, S.A. (2020). The use of cement treated reclaimed asphalt pavement-quarry waste blends as highway material. International Journal of Pavement Engineering, 21(10): 1191-1198. https://doi.org/10.1080/10298436.2018.1530445

[7] Jia, Y., Yang, Y., Liu, G., Gao, Y., Yang, T., Ding, F. (2019). Analysis of flexural fatigue failure and

degradation reliability of cement concrete for highway pavements. In CICTP 2019, pp. 951-963.

[8] Shalabi, F. I., Mazher, J., Khan, K., Alsuliman, M., Almustafa, I., Mahmoud, W., Alomran, N. (2019). Cement-stabilized waste sand as sustainable construction materials for foundations and highway roads. Materials, 12(4): 600. https://doi.org/10.3390/ma12040600

[9] Andika, M.H., Endawati, J. (2019). Mechanical properties of pervious concrete with slag and silica fume as cement substitution for highway shoulder. In IOP Conference Series: Materials Science and Engineering, 508(1): 012062. https://doi.org/10.1088/1757-899X/508/1/012062

[10] Zhang, T., Ren, Y. (2019). Identification and detection of a void under highway cement concrete pavement slabs based on finite element analysis. Rudarsko-Geološko-Naftni Zbornik, 34(3): 41-47. https://doi.org/10.17794/rgn.2019.3.5

[11] Oluwatuyi, O.E., Adeola, B.O., Alhassan, E.A., Nnochiri, E.S., Modupe, A.E., Elemile, O.O. (2018). Ameliorating effect of milled eggshell on cement stabilized lateritic soil for highway construction. Case Studies in Construction Materials, 9: e00191. https://doi.org/10.1016/j.cscm.2018.e00191

[12] Magee, B., Woodward, W.D.H., Tretsiakova-McNally, S., Lemoine, P. (2018). A preliminary investigation into geopolymer cement mortar's suitability for providing resilient highway solutions. In Sixth International Conference on the Durability of Concrete Structures. 170-177, 6th International Conference on Durability of Concrete Structures, ICDCS 2018.

[13] Vu, P.T.A. (2016). Ground improvement using soil-cement method: a case study with laboratory testing and in-situ verification for a highway project in southern Vietnam. Geotechnical Engineering Journal of the SEAGS & AGSSEA, 47(1): 45-49.

[14] Xue, Y.Q., Ding, F., Chen, F.L., Shi, X.W., Zhu, G.J. (2014). Fatigue damage reliability analysis of cement concrete for highway pavement. Jianzhu Cailiao Xuebao/Journal of Building Materials, 17(6): 1009-1014. https://doi.org/10.3969/j.issn.1007-9629.2014.06.012

[15] Edeh, J.E., Ashanda, T.O., Osinubi, K.J. (2014). Effect of cement on palm kernel shell ash stabilized reclaimed asphalt pavement as highway pavement material. In Pavement Materials, Structures, and Performance, 29-38. https://doi.org/10.1061/9780784413418.004

[16] Peng, X. (2022). Recycling technology of old cement concrete pavement in highways. Vibroengineering PROCEDIA, 46: 86-91. https://doi.org/10.21595/vp.2022.22957

[17] Zhu, Z., Chen, X. (2022). Discussion and analysis on the improvement of the widening technology of cement concrete pavement of rural highway. European Journal of Remote Sensing, 55(sup1): 24-34. https://doi.org/10.1080/22797254.2022.2031305

[18] Edeh, J.E., Joel, M., Ogbodo, V.O. (2022). Effects of oil palm fibre ash on cement stabilised lateritic soil used for highway construction. International Journal of Pavement Engineering, 23(3): 834-840. https://doi.org/10.1080/10298436.2020.1775230

[19] Zhang, Y., Liu, G., Wang, Z., Du, H. (2022). Study on influencing factors of bond performance between cement concrete pavement and overlay layer in highway tunnel. In Sixth International Conference on Electromechanical Control Technology and Transportation (ICECTT 2021) 12081: 332-338. https://doi.org/10.1117/12.2623972

[20] Ta, D.T., Nguyen, T.D., Nguyen, D.M., Pham, V.H., Bui, A.T. (2022). Study on Application of Sea Sand-Cement Column in Soft Soil Improvement for Hai Phong-Nam Dinh Coastal Highway. In CIGOS 2021, Emerging Technologies and Applications for Green Infrastructure: Proceedings of the 6th International Conference on Geotechnics, Civil Engineering and Structures, 1191-1199. https://doi.org/10.1007/978-981-16-7160-9_121

[21] Ademila, O. (2021). Engineering characteristics of cement-stabilized lateritic soils for highway construction. In Recent Advances in Environmental Science from the Euro-Mediterranean and Surrounding Regions (2nd Edition) Proceedings of 2nd Euro-Mediterranean Conference for Environmental Integration (EMCEI-2), Tunisia 2019, pp. 271-278. https://doi.org/10.1007/978-3-030-51210-1_45

[22] Churchill, C.J., Panesar, D.K. (2013). Life-cycle cost analysis of highway noise barriers designed with photocatalytic cement. Structure and Infrastructure Engineering, 9(10): 983-998. https://doi.org/10.1080/15732479.2011.653574

[23] Yu, L.H., Zhou, S.X., Deng, W.W. (2013). Evaluation on Quality of Cement Concrete in Pavement of Highway. In Advanced Materials Research, 717: 295-300. https://doi.org/10.4028/www.scientific.net/AMR.717.295

[24] Zou, P., Huang, Z.Q., Tong, Y., Tan, L.C., Li, R., Wei, K., Qiao, D. (2022). Experimental evaluation of the mechanical properties of cement sheath under high-temperature conditions. Fluid Dynamics and Materials Processing, 18(3): 689-699.

[25] Gunjal, S.M., Kondraivendhan, B. (2022). High temperature impact on calcined clay-limestone cement concrete (LC3). Materials Today: Proceedings, 61: 386-391. https://doi.org/10.1016/j.matpr.2021.10.300

[26] Duarte, A.P., Rosa, I.C., Arruda, M.R., Firmo, J.P., Correia, J.R. (2022). Fire Behaviour of GFRP-Reinforced Concrete Slab Strips: Fire Resistance Tests and Numerical Simulation. In 10th International Conference on FRP Composites in Civil Engineering: Proceedings of CICE 2020/2021 10, 788-800. https://doi.org/10.1007/978-3-030-88166-5_68

[27] Ye, Z., Heidarpour, A., Jiang, S., Li, Y., Li, G. (2022). Numerical study on fire resistance of cyclically-damaged steel-concrete composite beam-to-column joints. Steel and Composite Structures, 43(5): 673. https://doi.org/10.12989/scs.2022.43.5.673